Dynamics of vertical-Bloch-line clusters

M. V. Chetkin, V. B. Smirnov, A. F. Novikov, I. V. Parygina,
A. K. Zvezdin, and S. V. Gomonov

Moscow State University
(Submitted 3 February 1988)
Zh. Eksp. Teor. Fiz. **94**, 164–173 (November 1988)

The dynamics of vertical Bloch line (VBL) clusters in domain walls of yttrium iron garnet films with uniaxial anisotropy perpendicular to the film plane is investigated by a two-photograph method. It is shown that a VBL cluster on a moving domain wall is accompanied by a solitary flexural wave of the wall. It is established that in the presence of large dissipation the solitary wave is asymmetric, viz., its leading front is steeper and its trailing edge is elongated. With an increase in the number of VBL in the cluster the amplitude of the solitary flexural wave slope of its leading front increases, and starting with a certain amplitude it becomes similar in shape to the profile of a shock wave. The cluster velocity decreases when the number of BFL in it increases. It is shown that the cluster is set in motion by a gyroscopic force. The profiles of the isolated flexural waves of the domain wall are calculated for large and small amplitudes. The calculated and experimentally observed profiles of these waves are compared. The number of BFL in the clusters is estimated. It is shown that for an adequate description of the profiles of the solitary flexural waves accompanying the moving BFL clusters account must be taken of the curvature and of the nonlinear dependence of the azimuthal angle of the magnetization at the center of the domain wall.

1. INTRODUCTION

Vertical Bloch lines (VBL) demarcate sections with different magnetic-moment rotation directions in Bloch domain walls (DW) of ferromagnets.[1] Under static conditions, these lines were observed by transmission electron microscopy[2] and by the Kerr effect.[3] Necking (Néel sections of Bloch DW) was observed in Ref. 4. Resonant VBL oscillations and the connection between the dynamics of broad DW and VBL in yttrium iron garnet slabs having low cubic anisotropy were investigated in Ref. 5. The frequency spectrum of DW with VBL in epitaxial iron-garnet films were investigated in Ref. 8. A method of rocking DW by a high-frequency field to find the positions of VBL was used in Ref. 7.

The dynamic properties of VBL in epitaxial iron-garnet film having large uniaxial anisotropy are of undisputed interest, especially in connection with plans to produce superdense (10^8–10^9 bit/cm^2) magnetic memories.[8] It is known that as VBL move along a DW flexure of the latter can result from the action of the gyrotropic force. It follows from the theory that a VBL is accompanied by a solitary flexural wave.[9-11] Such a flexural wave makes it possible, in particular, to observe and investigate the dynamics of VBL. Note that the amplitude of a flexure produced by a single VBL is small in typical iron garnets (less than 0.5 μm according to calculations), and this is one of the difficulties encountered in experimental investigations of VBL dynamics. The amplitude of the DW flexure can be increased by decreasing the degree of spin "twisting." It is possible to produce artificially on DW formations (see below) with the spin twisted by $N\pi$, where N is an integer. Such a formation is called a VBL cluster, bearing it in mind that under certain conditions moving VBL tend to be bunched. Obviously, a moving cluster produces, other conditions being equal, a larger flexure and influences more strongly the DW dynamics. A similar procedure was used in experiments[12-14] on VBL clusters in epitaxial iron-garnet films.

An important manifestation of DW flexure is a contribution, nonlinear in the velocity, to the VBL retarding force.[11] The presence of this additional damping is important also for isolated VBL. Its manifestation is even stronger in the dynamics of the clusters.

In the present paper, which is a continuation of Ref. 13, we investigate theoretically and experimentally the dynamics of VBL clusters in epitaxial iron-garnet films with large uniaxial anisotropy, and in particular the dependence of the cluster velocity on the DW velocity and on the number of VBL in the cluster.

2. EXPERIMENT

A high-speed two-photograph method[13,15] was used to record the DW dynamic profiles and to determine the VBL cluster velocity in real time. The only straight wall in the investigated $(BiLaTm)_3(FeGa)_3O_{12}$ iron garnet sample was produced by a magnetic field perpendicular to the sample surface and having a gradient 1500 Oe/cm in a direction perpendicular to the DW. An epitaxial film 7 μm thick, with domain size 47 μm, quality parameter $Q = 45$, saturation magnetization $4\pi M_s = 100$ G, and a single statically straight wall was placed in a pulsed magnetic field perpendicular to the film plane; this field set the DW in motion.

Light pulses from two LGI-21 lasers triggered by two pulse generators at an adjustable delay between them were used for optical pumping of the dye rhodamine 6G. This resulted in pulses of yellow light of 8 ns duration. These pulses were applied through an optical system to the sample, which was located on the object stage of a microscope, and from there to a photographic camera with high-sensitivity film. The optical resolution of the system was not worse than 0.5 μm, owing to the use of an objective with 60× magnification. The need for high magnification required the microscope objective to be close to the surface of the investigated iron-garnet film. A gradient magnetic field was therefore

 0038-5646/88/112269-05$04.00

produced by two permanent magnets placed directly below the substrate on which the investigated film was grown, with opposite poles in contact with the substrate. This produced a planar magnetic-field component in the investigated samples, and made the Slonczewski peak [16] observable on the $v(H)$ plot of the DW velocity vs the field. Clusters containing various numbers of VBL could be produced by making current pulses of duration 20 to 100 ns and amplitude up to hundreds of milliamperes flow through a conductor parallel to the sample and making an angle with the DW, or through a thin loop deposited by photolithography on the sample in a direction perpendicular to the DW.

3. EXPERIMENTAL RESULTS

We investigated the non-one-dimensional dynamics of a DW in iron-garnet films whose anisotropy was perpendicular to the film plane. Figure 1 shows sets of paired high-speed domain-contrast photographs of the dynamic domain structure in the investigated samples. Each pair (Figs. 1a–d) shows clearly two positions of the downward moving DW, separated by a time interval Δt. The dark stripe is the region traversed by the DW during the time between the two light pulses. The photographs show clearly non-one-dimensional asymmetric formations that lag the DW and move along it. These are the solitary flexural waves of the wall, which accompany the VBL clusters moving along the dynamic DW. The profile of the solitary wave is asymmetric: the leading front is steeper and the trailing one is elongated. The slope of the solitary-wave leading front increases with increase of the wave amplitude and of the DW velocity.The amplitude of the solitary wave on Fig. 1a is 1.5 μm and its velocity is three times that of the DW.

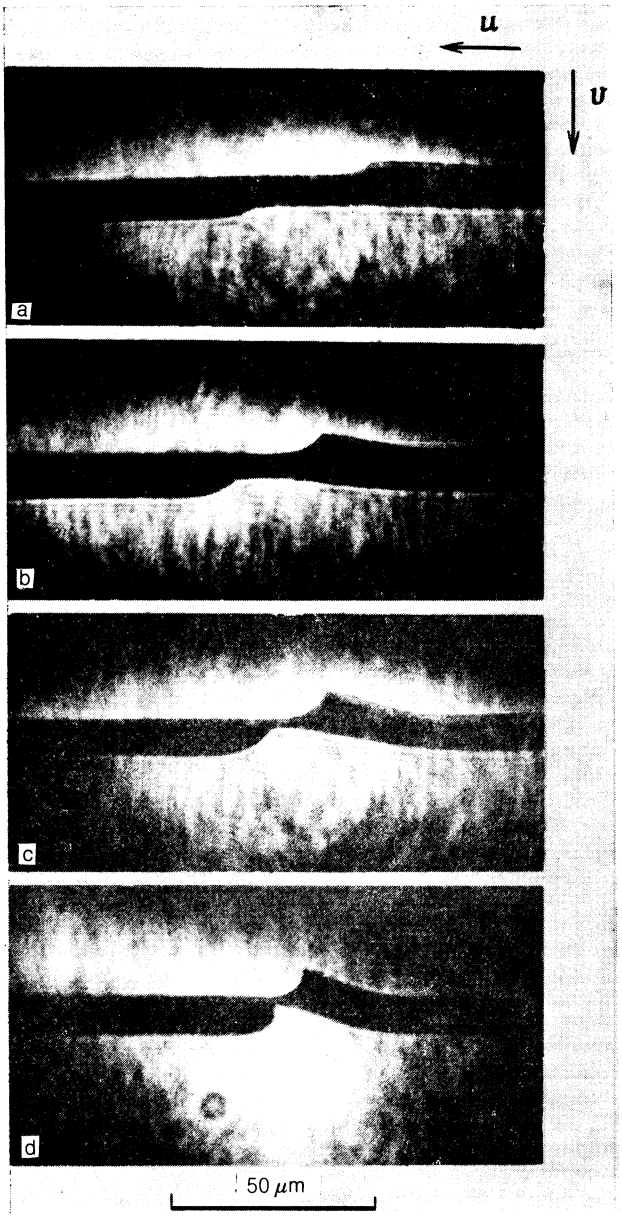

FIG. 1. Series of double high-speed photographs of dynamic domain structures in an epitaxial iron-garnet film for different amplitudes of solitary waves moving along a domain wall; time delay $t = 0.5\,\mu$s (a,b,c) and $0.35\,\mu$s (d).

When the solitary-wave amplitude is increased, the discontinuity of the spatial derivative on the leading front becomes distinctly visible (Figs. 1b and 1c). With further increase of its amplitude, the solitary wave profile changes substantially: the leading front acquires a region with a vertical tangent, which becomes more stongly pronounced with increase of the DW velocity (Fig. 1d). In Figs. 1a–1c the DW velocity is $v = 20$ m/s and the Slonczewski peak velocity is $v_p = 30$ m/s, while in Fig. 1d $v = 30$ m/s and $v_p = 55$ m/s. Behind the leading front is a plateau which is particularly noticeable at large amplitudes of the solitary wave. As the amplitude of the solitary wave increases, the size of the DW flexure decreases. The solitary-wave profile is then similar to that of a shock wave. The small change of the shape of the dynamic profile of the solitary wave in the second (lower, see Fig. 1d) position of the dynamic DW, is due to the existence of a gradient magnetic field that stabilizes the isolated DW in the sample.

The profiles of solitary waves at DW velocities from 3 to 20 m/s are similar. Solitary waves with amplitudes up to 10 μm are stationary, and are observed in the experiment during the entire time of their motion of the DW. The direction of a solitary wave along a DW depends on the direction of the velocity vector of the latter. This confirms that the VBL cluster is set in motion by the gyroscopic force.

Figure 2 shows experimental and theoretical (see Sec.

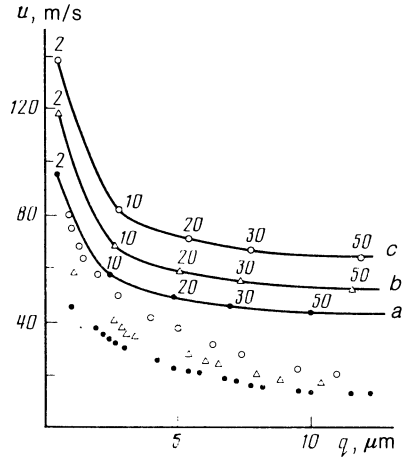

FIG. 2. Velocities of solitary flexural DW waves accompanying a VBL cluster vs their amplitudes. The experimental data were obtained at DW velocities 11 m/s (●), 15 m/s (△), and 20 m/s (○); *a,b,c*—respective theoretical dependences at the same DW velocities. The numbers on the theoretical curves are the numbers, corresponding to the given DW flexure amplitude, of Bloch lines in the cluster.

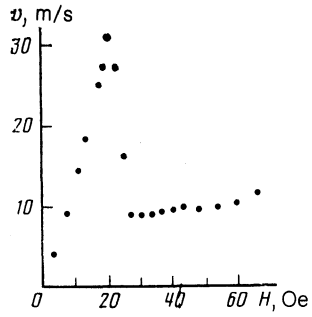

FIG. 3. DW velocity vs the magnetic field.

4) dependences of the VBL cluster velocities on the solitary-wave amplitude, for DW having velocities 11, 15, and 20 m/s. The minimum solitary-wave amplitude observed in our experiment was 0.8 μm. In this case, at a DW velocity 20 m/s, the VBL cluster had a maximum velocity 80 m/s. This is much lower than the limit calculated for one VBL, but on the other hand several times higher than the maximum velocity observed in Ref. 14 for one VBL, as stated there. Neither the DW flexure size nor photographs similar to Fig. 1 are contained in Ref. 14. It seems that the experiment was performed there with a cluster of several VBL, and the cluster velocity limit is substantially lower than for a single VBL. When the amplitude of a solitary wave is increased, its velocity, as seen from Fig. 2, approaches the DW velocity.

Figure 3 shows the dependence of the DW velocity on the pulsed field H in the investigated sample. The Slonczewski peak[16] is distinctly observed at $H = 20$ Oe. The peak is due to the appearance of horizontal Bloch lines (HBL) and of VBL in the moving DW, and this decreases substantially the DW mobility. We have determined the VBL cluster velocity on the linear section of the $v(H)$ plot for DW at velocities lower then v_p. When the magnetic field is increased above 20 Oe, VBL clusters are produced in the entire DW, and structures are formed in it.[17] The latter interact with one another and with the clusters produced with the aid of the current loop, making their identification and a determination of their velocity difficult. The $v(H)$ dependence yields for the investigated sample a DW mobility $\mu = 140$ cm/s·Oe and damping parameter $\alpha = 0.38$; the latter is needed for the theoretical analysis.

Keeping constant the current and the pulse duration in the loop that creates the VBL cluster, we were able to obtain the dependence of the velocity of the isolated wave accompanying this VBL cluster on the magnetic field that moves the DW. This dependence is shown for a solitary wave of minimum size in Fig. 4. It can be seen that at $H = 16$ Oe the VBL cluster velocity u does not reach its limiting value, and the VBL cluster mobility $\mu_{BL} = 600$ cm/s·Oe is much higher than the DW mobility. To determine the VBL cluster velocity limit one must use stronger magnetic fields, in which it is difficult to prevent creation of additional VBL along the entire DW past the Slonczewski peak.

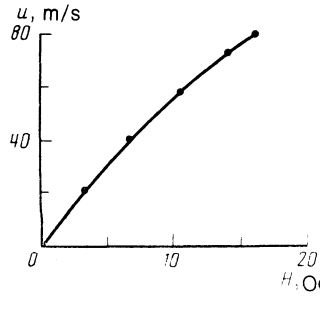

FIG. 4. Velocity of solitary wave accompanying a VBL cluster as a function of the magnetic field.

We were unable to determine directly from experiment the number of VBL in the cluster. This calls for invoking the results of a theoretical analysis and for interpreting on its basis the dependence of the VBL cluster velocity on the amplitude of the accompanying solitary wave.

4. DISCUSSION OF RESULTS

In the discussion of the experimental data we proceed from Ref. 11, where the nonlinear dynamics of a solitary VBL is described in terms of the coordinate of its center and of the momentum, i.e., as a material point. To extend this description to include a cluster, we present the basic equation of stationary motion of a VBL in a notation that differs somewhat from that used in Ref. 11. The gyroscopic force f_g (Ref. 16) causing the VBL motion is

$$f_g = \frac{2M_s}{\gamma} vh\delta\psi,$$

where h is the film thickness, γ the gyromagnetic ratio, $\delta\psi = \psi(\infty) - \psi(-\infty)$ and the total increase of the angle on going through the VBL (cluster). For VBL we have $\delta\psi = \pi$ and for a cluster $\delta\psi = N\pi$. There are two dissipative forces. The first is due to the energy lost by spin precession in the VBL itself. For a VBL it is equal to

$$f_d^{(1)} = \frac{2M_s u}{\mu_{BL}} = \frac{2M_s}{\gamma} uh\alpha\Delta \int_{-\infty}^{\infty} \left(\frac{\partial\psi}{\partial x}\right)^2 dx,$$

where μ_{BL} is the VBL mobility, α is the dimensionless damping constant in the Landau-Lifshitz equations (in the Gilbert form), $\Delta = (A/K_u)^{1/2}$ is the DW thickness (A is the exchange interaction constant and K_u is the uniaxial anisotropy constant). On going from a VBL to a cluster this equation remains in force on substitution of the appropriate function $\psi(x)$ that describe the VBL cluster. The source of the second dissipative force $f_d^{(2)}$ is the DW "moving flexure" $q(x,t)$. It can be calculated in the following manner. A moving-DW area element $h\delta q$ is acted upon by a viscous retarding force

$$h\delta q \frac{2M_s}{\mu_w}(\dot{q}\mathbf{x}^0) = \frac{2M_s}{\mu_w} u \frac{\partial q}{\partial x} h \frac{\partial q}{\partial x} dx, \qquad (1)$$

where $\mu_w = \gamma\Delta/\alpha$ is the DW mobility, and $\mathbf{x}^0$ is a unit vector along the x axis. Integrating (1), we obtain

$$f_d^{(2)} = \frac{2M_s\alpha hu}{\gamma\Delta} \int_{-\infty}^{\infty} \left(\frac{\partial q}{\partial x}\right)^2 dx.$$

For stationary VBL motion, the gyroscopic moving force is balanced by the viscous retardation forces

$$v\delta\psi = \alpha\Delta u \left[\int_{-\infty}^{\infty} \left(\frac{\partial\psi}{\partial x}\right)^2 dx + \frac{1}{\Delta^2}\int_{-\infty}^{\infty} \left(\frac{\partial q}{\partial x}\right)^2 dx\right]. \qquad (2)$$

The flexure function $q(x)$ is defined by the expression [11]

$$q(x)=u\int_{-\infty}^{\infty}G(x-\xi)\frac{\partial\psi}{\partial\xi}d\xi, \tag{3}$$

where the Green's function is given by

$$G(x)=\frac{\Delta}{\Lambda_+-\Lambda_-}\begin{cases}\exp\left(-\dfrac{|\Lambda_-|}{\Delta_L}x\right), & x>0\\ \exp\left(\dfrac{|\Lambda_+|}{\Delta_L}x\right), & x<0\end{cases},$$

$$\Lambda_\pm=-\alpha u/2S\pm[(\alpha u/2S)^2+b^2]^{1/2}.$$

Here $b^2=H_z'\Delta/4\pi M_s,H_z'$ is the magnetic-field gradient, $\Delta_L=(A/2\pi M_s^2)^{1/2}$ is the VBL thickness, and $S=\gamma(8\pi A)^{1/2}$.

We call attention to the fact that if dissipation is taken into account the leading front of the flexure wave $q(x-ut)$ is steeper (with a slope $1/|\Lambda_-|$) than the trailing edge (with slope $1/|\Lambda_+|$), as is clear from experiment (Fig. 1). Thus, to calculate the velocity of a VBL (or a cluster) it suffices to specify the function $\psi(x)$. This function is determined jointly with $q(x)$ by the Slonczewski equations. Reference 11 contains a consistent procedure for calculating $\psi(x)$ and $q(x)$ for a solitary VBL. We have no such solution for a VBL cluster. We confine ourselves here therefore to the use of the trial $\psi(x)$ function usually employed to describe rigid magnetic bubble domains[16]

$$\psi_\xi=\begin{cases}1/\Delta_L, & |\xi|<\pi N\Delta_L/2\\ 0, & |\xi|>\pi N\Delta_L/2\end{cases}. \tag{4}$$

Substituting (4) in (3) and (2) we get

$$\frac{Q^{1/2}\pi v}{2\alpha}=u\left\{1+\frac{u^2}{8A\gamma^2(b_++b_-)}\left[\frac{1-\exp(-\pi Nb_+)}{2\pi Nb_+}+\frac{1-\exp(-\pi Nb_-)}{2\pi Nb_-}-(\exp(-\pi Nb_-)-\exp(-\pi Nb_+))/\pi N(b_+-b_-)\right]\right\}, \tag{5}$$

where

$$b_\pm=(b^2+(\alpha u)^2/32\pi A\gamma^2)^{1/2}\pm\alpha u/\gamma(32\pi A)^{1/2}.$$

If $u\ll\gamma(8\pi A)^{1/2}$ and $N\ll(\pi b_\pm)^{-1}$ Eq. (5) goes over into the known relation obtained by Slonczewski.[16]

With increase of the number N of lines in the cluster, the $u(v)$ dependence becomes nonlinear. Figure 5 shows plots of

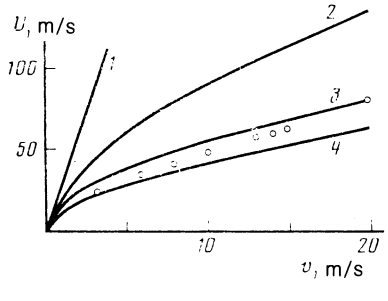

FIG. 5. Dependences of VBL cluster velocity on the DW velocity, calculated for $N=1$ (1), 2 (2), 10 (3), and 50 (4); ○—experimental values of minimum-amplitude clusters.

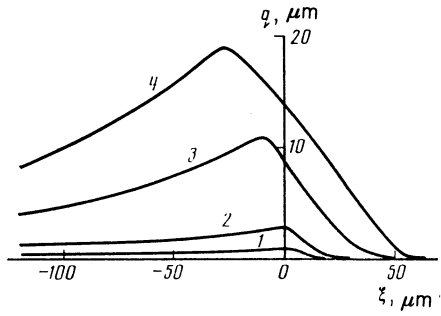

FIG. 6. Profiles of solitary waves propagating along DW, calculated for $N=2$ (1), 10 (2), 50 (3), 100 (4); $Q=45$, $4\pi M_s=100$ G, $H'=1500$ Oe/cm, $A=2.5\cdot10^{-7}$ erg/cm, $h=7$ μm, $b=0.01$, $\alpha=0.4$, and $\gamma=1.8\cdot10^7$ s$^{-1}\cdot$Oe^{-1}.

$u(v)$, based on Eq (5), for different N. The following material parameters were used in the calculation: $4\pi M_s=100$ G, $Q=45$, $\gamma=1.8\cdot10^7$ s$^{-1}\cdot$Oe^{-1}, $A=2.5\cdot10^{-7}$ erg/cm, $H_z'=1500$ Oe/cm, and $\alpha=0.4$ (these are the values for one of the investigated samples). Figure 5 shows also Slonczewski's result[16] for $N=1$. It has been found that as N increases the deviation of $u(v)$ from linearity first increases up to $N\approx60$, and begins to decrease for $N>60$. The cause of this behavior of $u(v, N)$ is that initially the increase of the number of VBL in the cluster leads to a rapid increase of the amplitude of the isolated wave (Fig.6) and of $\partial q/\partial x$ on the leading front. For $N>2/\pi b$ the amplitude begins to stabilize, $\partial q/\partial x$ decreases, and the relative contribution to the dissipative processes connected with the term $(\partial q/\partial x)^2$ in (2) again decreases. This may explain the results of Lian and Humphrey,[12] who state that larger clusters have higher velocities. It must be noted here, to be sure, that they did not determine directly the cluster velocities.

Figure 5 shows also the experimental values of $u(v)$ for minimum-N clusters observed in a dynamic experiment. These values of $u(v)$ were obtained from the data of Figs. 3 and 4. Comparing the theoretical and experimental $u(v)$ dependences we can conclude that experiment yields $N\approx10$ (especially at a DW velocity $v=20$ m/s). It is of interest to compare the solitary wave profiles and amplitudes obtained from the theory (Figs. 6 and 7) and from experiment (Fig. 1). It follows from this experiment that the derivative

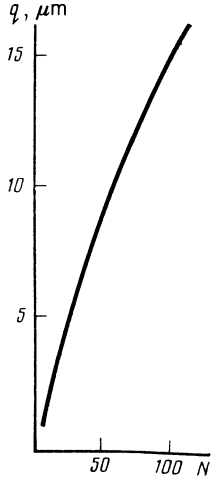

FIG. 7. Theoretical dependence of the amplitude of a solitary DW flexural wave on the number of VBL in a cluster.

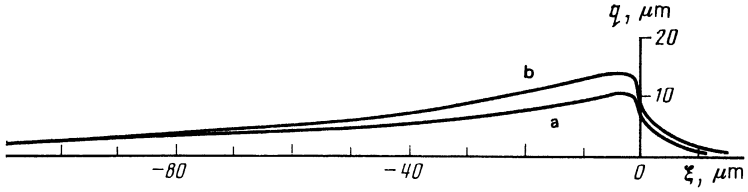

FIG. 8. Solitary DW flexural wave profiles numerically calculated from (6) and (7) for $\alpha = 0.2, A = 10^{-7}$ erg/cm, $4\pi M_s = 60$ G, $Q = 30$, $H' = 1500$ Oe/cm, and $v = 20$ m/s. a) $N = 35$, $u = 50$ m/s; b) $N = 50$, $u = 40$ m/s.

$\partial q/\partial x$ on the leading front is several times larger in experiment than in theory even at low amplitudes of the solitary waves. At high amplitudes this difference increases. It is possible that for a more adequate description of the leading front of a solitary wave it is necessary to take magnetostatic interactions into account.

The cause of the disparity of the forms of larger amplitude solitary waves may be that expression (2) and the ensuing (5) are valid only for large deviations of the DW form from planar, i.e., for $(\partial q/\partial x)^2 \ll 1$, which is correct if $N \ll 2\gamma(AK_u)^{1/2}/\pi \cdot M_s u$. For $u \sim 10$ m/s this condition is violated when N is more than several times ten. From a comparison of the minimum solitary-wave amplitude observed in experiment (Fig. 2) with its calculated values (Fig. 7) it follows that $N \approx 2$ in this case. The estimate of the number of VBL in a cluster, obtained by us by two methods, yields thus a mean value $N \approx 4$ or 6.

Figure 2 shows theoretical plots of $u(q)$ for different DW velocities. Comparing them with experimental data in the same figure we see that they are in qualitative agreement if it is assumed that the number of VBL in the clusters ranges from 2 to 60 (see Fig. 7). The experimental curves lie lower, by a factor 2–3, than the theoretical, and the decrease of u with increase of q is stronger in experiment than in theory. This may be again due to the strong increase of $(\partial q/\partial x)^2$ on the leading front of the solitary wave, which increases the contribution to the dissipation in accordance with (2).

The theory linear in q is no longer valid if $(\partial q/\partial x) \gtrsim 1$. It can be consistently generalized in this case on the basis of solutions of the nonlinear equations of DW motion:

$$\frac{1}{4\pi M\gamma\Delta}\frac{\dot q}{[1+(\partial q/\partial x)^2]^{1/2}} = \frac{1}{2}\sin\left(2\left(\psi - \operatorname{arctg}\left(\frac{\partial q}{\partial x}\right)\right)\right) - \frac{\Delta_L^2}{[1+(\partial q/\partial x)^2]^{1/2}}\frac{\partial}{\partial x}\left\{\frac{\partial\psi/\partial x}{[1+(\partial q/\partial x)^2]^{1/2}}\right\} + \frac{\alpha\psi}{4\pi M\gamma},$$

$$\frac{\Delta\psi}{4\pi M\gamma} = -\frac{\alpha}{4\pi M\gamma}\frac{\dot q}{[1+(\partial q/\partial x)^2]^{1/2}} + \Delta_L^2\frac{\partial}{\partial x}\left\{\frac{\partial q/\partial x}{[1+(\partial q/\partial x)^2]^{1/2}}\right\} - bq^2 + \frac{H_z\Delta}{4\pi M}.$$

These equations generalize the known Slonczewski equations, since they take into account the change of the DW area as it moves. It is particularly important to take this effect into account in an analysis of the form of the front of a moving VBL cluster (see Fig. 1). Profiles of the solitary waves accompanying VBL clusters, calculated with the aid of (7) under the assumption that $\psi(x) = Bx^2 + Cx + D$, (Fig. 8) have slopes close to the vertical "plateau" on which $\partial q/\partial x \ll 1$ and whose length increases with increase of the number of lines in the cluster.

5. CONCLUSION

1. A cluster moving along a domain-wall, containing from several up to some tens of vertical Bloch lines, is stable and is accompanied by a solitary flexural domain-wall wave. If the dimensionless damping parameter is large, the solitary wave is asymmetric with a steep leading front and an elongated trailing edge.

2. For large clusters and domain-wall velocities, the profile of the solitary wave is reminiscent of a shock wave.

3. The velocity of a cluster of vertical Bloch lines decreases with increase of the number of lines in it and tends then to reach the domain-wall velocity.

4. The experimental dependences of a VBL cluster velocity on the amplitude of the accompanying DW flexure solitary wave are qualitatively described by the Slonczewski equations with a linear dependence of the azimuthal magnetization angle at the DW center.

5. We have proposed for the Slonczewski equations a nonlinear generalization that is valid for large curvatures of the domain wall. This generalization describes qualitatively the profiles of the solitary waves that accompany a VBL cluster with a large number of lines.

[1] H. J. Williams and M. Goertz, J. Appl. Phys. **23**, 316 (1952).
[2] P. J. Grundy and S. R. Herd, Phys. Stat. Sol. **9**, 79 (1972).
[3] G. S. Krinchik and O. M. Benidze, Zh. Eksp. Teor. Fiz. **67**, 2170 (1974) [Sov. Phys. JETP **40**, 1026 (1975)].
[4] A. S. Sigov and A. G. Shishkov, Thin Sol. Films, **10**, 363 (1972).
[5] V. S. Gornakov, L. M. Dedukh, V. I. Nikitenko, and V. T. Synogach, Zh. Eksp. Teor. Fiz. **90**, 2090 (1986) [Sov. Phys. JETP **63**, 1225 (1986)].
[6] V. G. Pokazan'ev, Yu. I. Yalyshev, K. I. Lukash, and G. R. Purashev, Pis'ma Zh. Eksp. Teor. Fiz. **41**, 21 (1985) [JETP Lett. **41**, (1985).
[7] T. Suzuki and M. Asada, IEEE Trans. **MAG22**, 784 (1986).
[8] S. Konishi, *ibid.* **MAG19**, 1838 (1983).
[9] K. Matsuyama and S. Konishi, *ibid.* **MAG20**, 1141 (1984).
[10] A. V. Nikiforov and E. B. Sonin, Pis'ma Zh. Eksp. Teor. Fiz. **40**, 325 (1984) [JETP Lett. **40**, 1119 (1984)].
[11] A. K. Zvezdin and A. F. Popkov, Zh. Eksp. Teor. Fiz. **91**, 1789 (1986) [Sov. Phys. JETP **64**, 1059 (1986)].
[12] M. R. Lian and P. B. Humphrey, J. Appl. Phys. **57**, 4065 (1985).
[13] M. V. Chetkin, V. B. Smirnov, I. V. Parygina, *et al.*, Pis'ma Zh. Eksp. Teor. Fiz. **45**, 597 (1987) [JETP Lett. **45**, 762 (1987)].
[14] G. Ronan, J. Theile, H. Krause, and. J. Engeman, IEEE Trans. **MAG23**, 2332 (1987).
[15] M. V. Chetkin and S. N. Gadetskii, Pis'ma Zh. Eksp. Teor. Fiz. **38**, 280 (1983) [JETP Lett. **38**, 308 (1983)].
[16] A. P. Malozemoff and J. C. Slonczewski, *Magnetic Domain Walls in Bubble Materials*, Academic, 1979. [Russ. Transl., Mir, 1972, p. 362.
[17] M. V. Chetkin, A. K. Zvezdin, S. N. Gadetskii, *et al.*, Zh. Eksp. Teor. Fiz. **94**, 269 (1988) [Sov. Phys. JETP **67**, No. 1, 151 (1988)]

Translated by J. G. Adashko